



Effect of soil structure interaction on the seismic response of piled supported structures

Mohamed Elsebaey^{1*}, Ibrahim A. El-Araby¹, Rami Bakr¹, A. G. Salama^{2,1}, Hytham Elwardany¹

¹ Civil Engineering Department, Faculty of Engineering, Delta University for Science and Technology, Gamasa, P.O. Box 11152, Egypt

² Civil Engineering Department, Faculty of Engineering at Shoubra, Benha University, Shoubra, P.O. Box 11629, Egypt

* Corresponding author.

E-mail: Mohamed.Elsebaei@deltauniv.edu.eg (Mohamed Elsebaey), Ibrahim.alarabi@deltauniv.edu.eg (Ibrahim A. El-Araby), ramibakr2000@yahoo.com (Rami Bakr), agsalama@hotmail.com (A. G. Salama), Drhythamelwardany@yahoo.com (Hytham Elwardany)

ABSTRACT: The presence of liquefiable soil poses significant challenges for earthquake-resistant structure design. A substantial portion of previous research has overlooked soil-structure interactions in their analyses. However, during intense seismic activity, soil nonlinearity and separation at the soil-foundation interface can profoundly affect piled supported structures' response. Therefore, this study employs direct time-domain analysis to appropriately incorporate soil nonlinearity. A finite element model was developed using PLAXIS 2D under plain strain conditions. The PM4Sand model, renowned for simulating liquefaction behaviour in sand layers, was selected to represent the liquefiable layer. Nonetheless, the PM4Sand model has limitations in accurately capturing initial stress conditions. To address this, the Hardening Soil model with small-strain stiffness (HSS) was integrated for precise determination of initial stresses within the soil profile. The El Centro earthquake was used as the input ground motion. The findings are presented in terms of the pore water pressure ratio. The study reveals higher pore pressure ratios for piled-raft foundations compared to raft foundations alone. This distinction diminishes with increasing foundation depth, likely due to reduced inertial forces at greater depths. This observation underscores the crucial importance of accounting for soil-structure interaction in foundation analysis for structures situated on liquefiable soils.

Key words: Liquefaction; Earthquake Waves; pile; PM4Sand; Numerical analysis.

1. Introduction

The seismic performance of structures is fundamentally influenced by soil-foundation-structure interaction (SSI) during earthquake events. Pile foundations are a prevalent choice in seismically active zones due to their enhanced

bearing capacity and control of settlements. However, the presence of liquefiable soil introduces significant complexities. Dynamic loads from both the structure itself and the surrounding soil act on the piles. Additionally, the nonlinear behaviour of the soil leads to a concurrent reduction in shear strength and a substantial degradation of stiffness over time due to pore pressure generation (López Jiménez, Dias, and Jenck 2019). Wilson 1998 examined the p-y response of piles embedded in liquefiable sands. Their research identified a pronounced time dependence within the p-y relationship for these soils. The tests revealed a diminishing trend in the pile's lateral resistance as pore water pressures increased. Notably, even under substantial relative displacements, the lateral resistance remained markedly low. Tokimatsu, Suzuki, and Sato 2005 investigated the influence of inertial and kinematic forces on pile behaviour. Their findings suggest that when the superstructure's natural period is shorter than the site period, kinematic forces become in phase with inertial forces, leading to amplified loads within the

piles. Conversely, when the periods are out of phase, the forces counteract each other. Several researchers have proposed simplified methodologies to analyse soil-pile-structure interaction (SPSI) in liquefiable soils. Yao et al. 2004 highlighted the critical role of the transient state preceding soil liquefaction in pile design. This emphasis stemmed from their observation that dynamic earth pressure reached its peak value during this transient phase. Ashour and Norris 2003 presented a novel approach to analyse the lateral response of an isolated pile embedded in liquefiable sand subjected to dynamic loading. Their procedure incorporates the integration of free-field and near-field pore water pressures within the framework of the strain wedge model. The results revealed a significant reduction in both the capacity and stiffness at the pile head, which can be attributed to the onset of liquefaction compared to the response observed under drained conditions. Other researchers such as, (Abdoun and Dobry 2002; Suzuki et al. 2006; Dungca et al. 2006; Bhattacharya, Madabhushi, and Bolton 2004; Tamura and Tokimatsu 2006; Han et al. 2007; R. W. Boulanger et al. 1999; Towhata et al. 1999; Horikoshi, Tateishi, and Fujiwara 1998; Takahashi 1998; T. H. Abdoun 1998; Dobry, Taboada, and Liu 1997; Satoh, Ohbo, and Yoshizako 1998) also investigated the dynamic behaviour of pile foundations in liquefiable soils based on physical model tests with centrifuge shakers or large shaking tables and numerical analyses.

2. Model Verification

The main goal of this section is to compare the accuracy of the nonlinear finite element model with existing studies. A dynamic model was examined to validate the reliability of the PLAXIS 2D V21 finite element model in analyzing the behaviour of structures under seismic excitation. Toma, 2017 developed a 2D finite element model to investigate the effect of piles founded in soft clay on the earthquake response of a structure. The results of this simulation helped to confirm the models used in this study.

2.1. Overview and Model Information

The Seismic response of the structures with shallow foundation is evaluated using 2D PLAXIS code. The overall dimensions and the model boundaries are shown in figure 1. The model was meshed by a 15-node triangular element under plain strain, where the out-of-plane strain is fixed and equal to zero. While, the lateral direction of the boundary is given a tied degree of freedom on both sides, but the vertical direction is maintained with typical fixities. The model consists of Two layers The upper layer is clay, 10m thickness the second layer is relatively dense sand with 15m thickness shown in Figure 1. An average shear wave velocity of the upper clay layer V_{s1} is taken as 100 m/s, while V_{s2} is taken as 148 m/s. More details on the parameters used to model the soil and structure can be found in (Toma 2017).

2.2. Earthquake Modeling

Earthquake is modelled as dynamic prescribed displacement in the x-direction at the bedrock level and the y-component is fixed, the earthquake is entered as a table of time - acceleration as shown in Figure (2).

2.3. Performing Calculations

The process of performing calculations is divided into multiple phases as shown in figure 3.

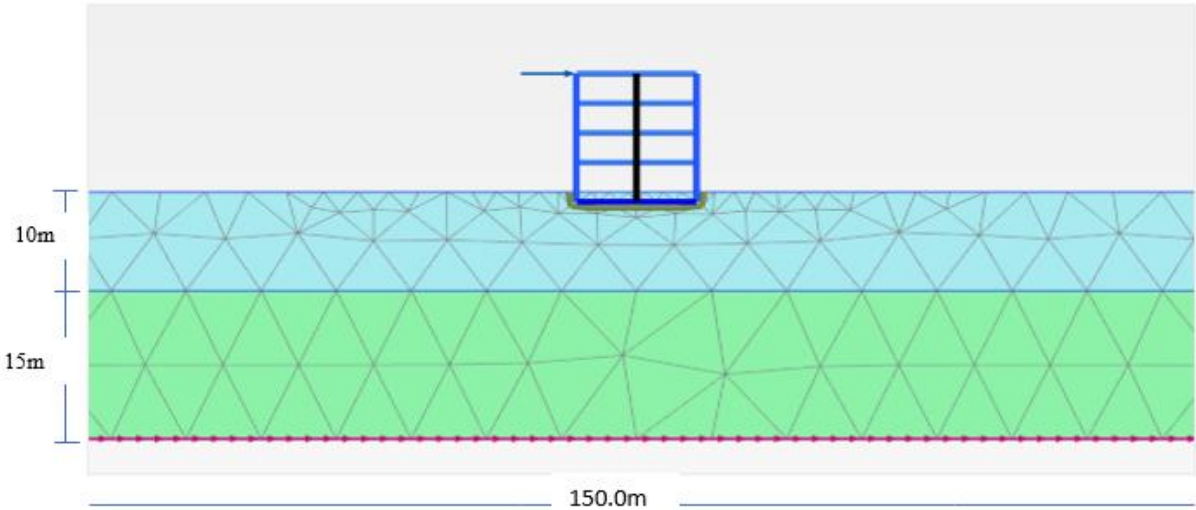


Figure 1. Plaxis 2D mesh used in numerical analysis.

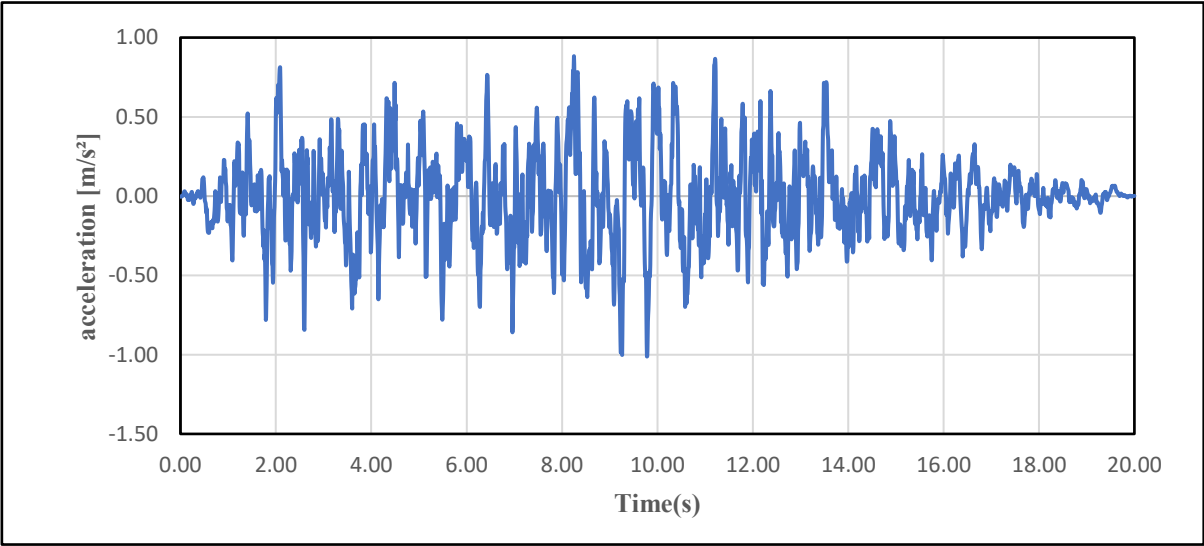


Figure 2. Earthquake acceleration-time records.

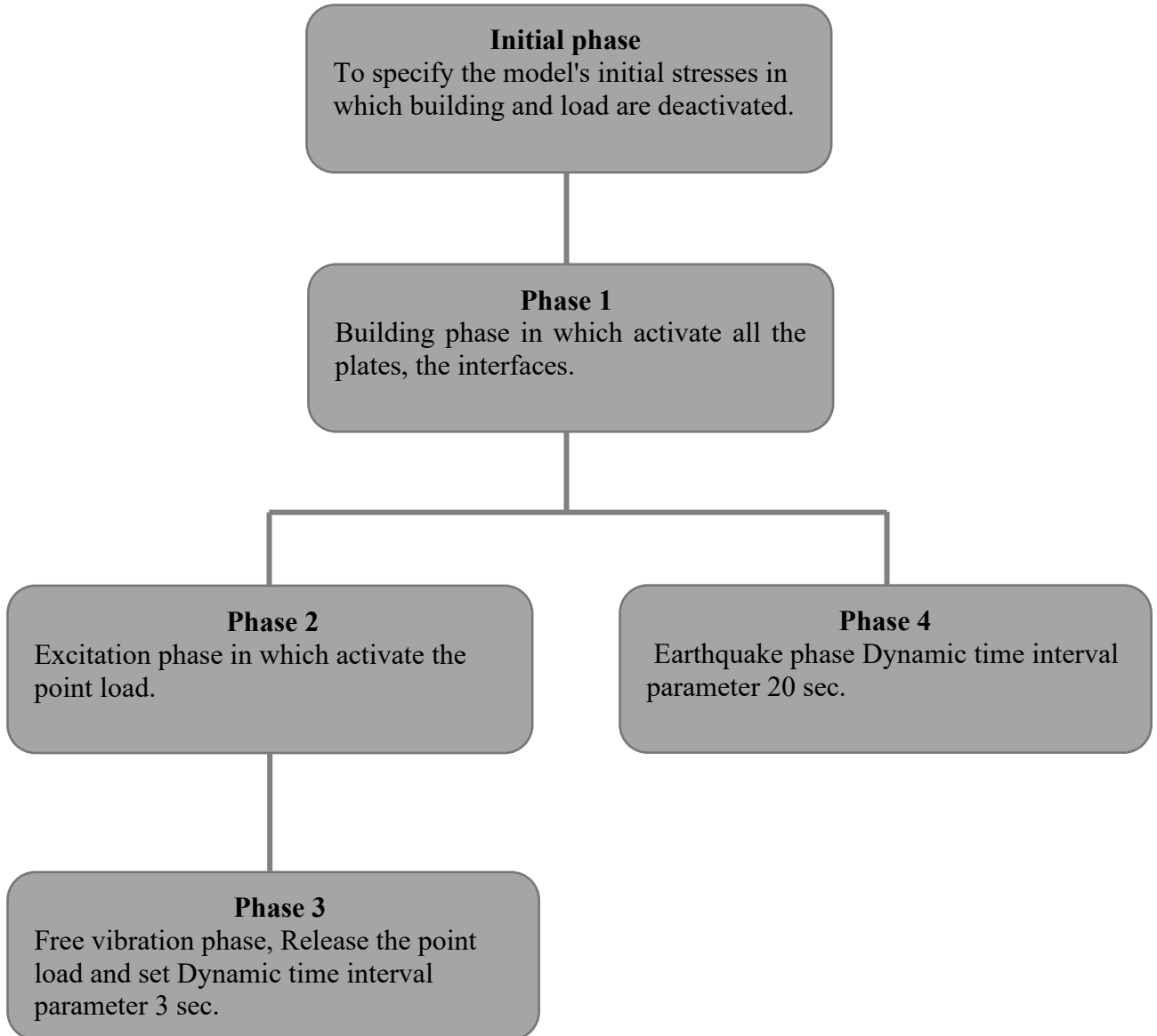


Figure 3. construction Stages used in Plaxis 2D.

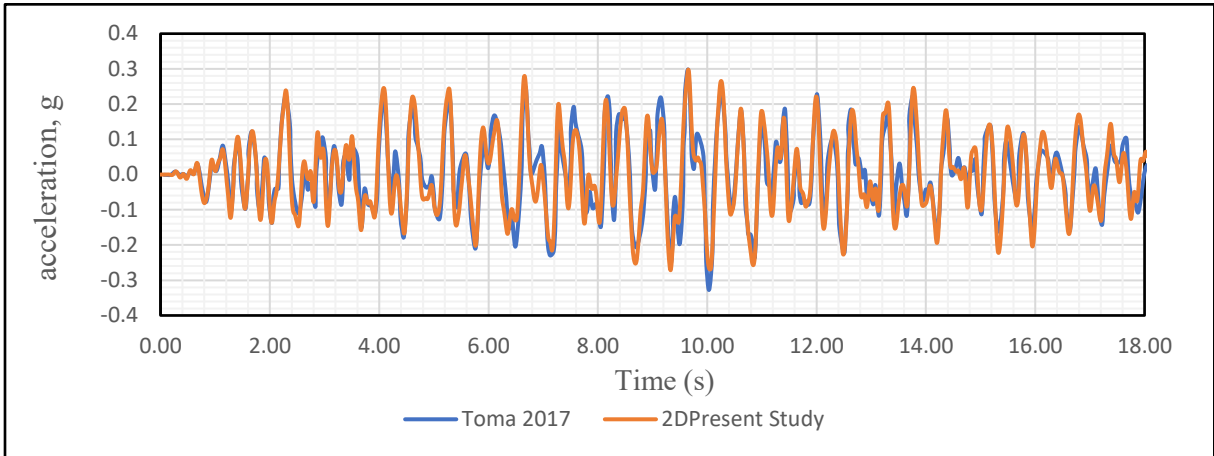


Figure 4. Comparison between PLAXIS 2D results of present study and results of (Toma 2017)

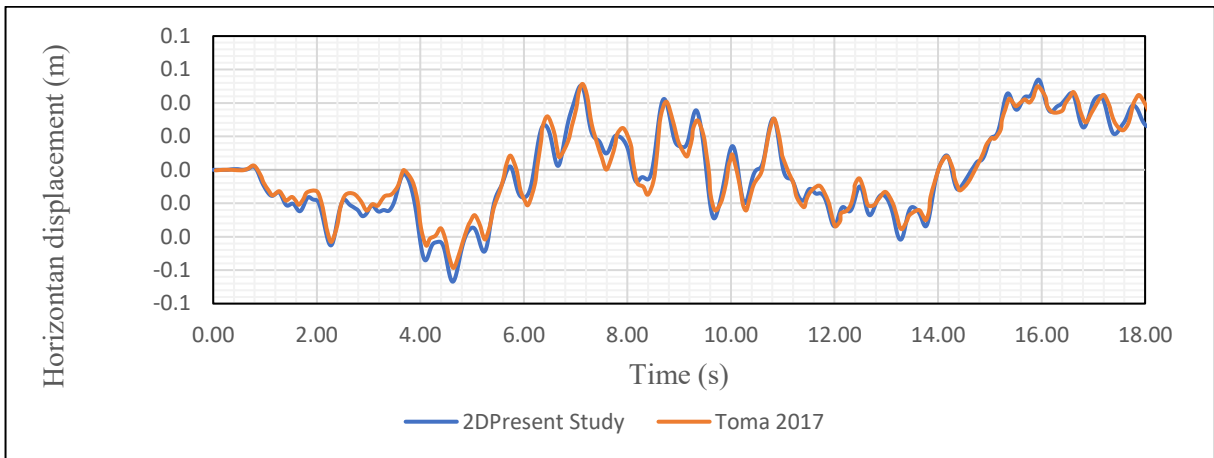


Figure 5. Comparison between PLAXIS 2D results of present study and results of (Toma 2017)

The numerical analysis, which covers the lateral acceleration, and lateral displacement of the stories in terms of trend and value, agrees well with the (Toma 2017) results in terms of trend and value.

3. Numerical study

3.1. Seismic input

The El-Centro earthquake record (north-south component) was selected as the input motion. This record represents an actual earthquake with a moment magnitude of 6.9, resulting in peak ground accelerations of 3.5 m/s^2 . The acceleration time history using this earthquake is shown in Figure 6.

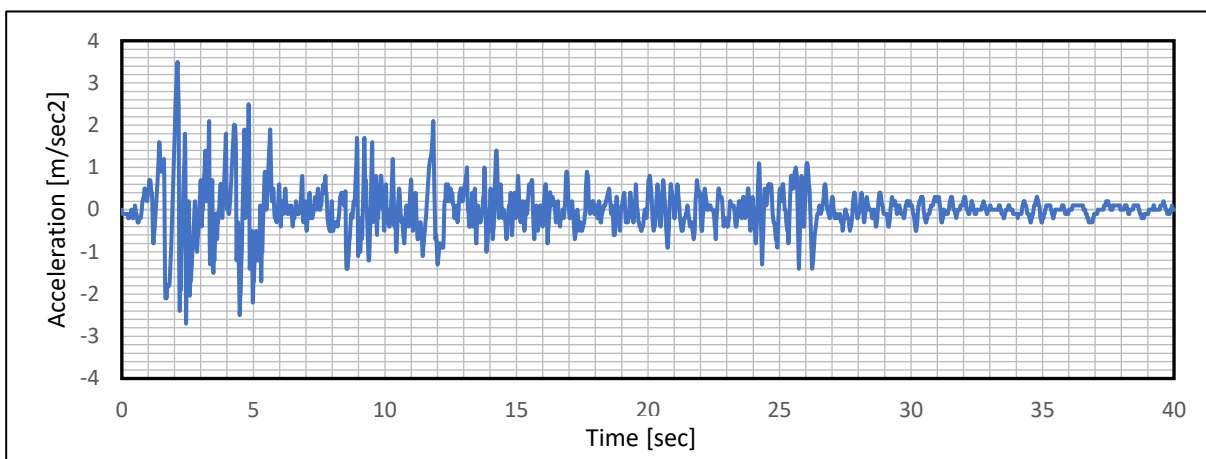


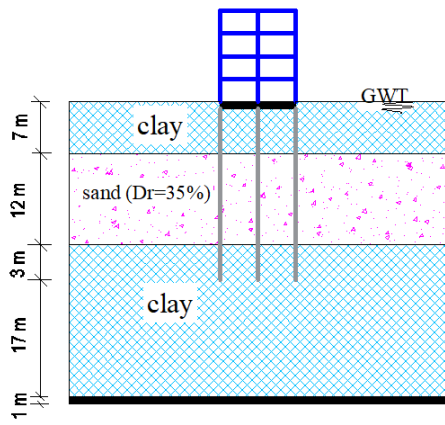
Figure 6. Acceleration-time histories of input earthquake

3.2. Geometry of the numerical model

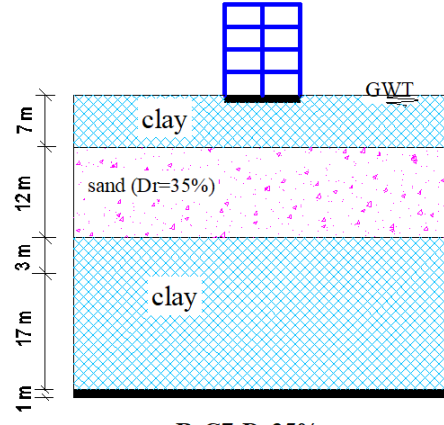
Twelve different soil profiles were simulated to thoroughly study the problem. Table 1 and Figure 7 provide a summary of the analysed geometries. The name of the case has three terms; the first term (RP or R) refers to Raft over pile or Raft only, the second one (C7 or C4) upper clay crust 7m or upper clay crust 4m, and the third term is the relative density of the liquefaction soil (Dr 35, 55, or 75 %).

Table 1. summary of analysed geometries

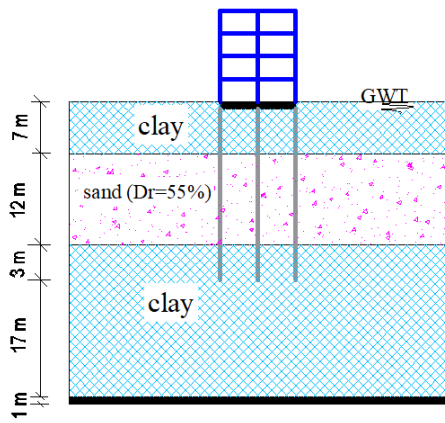
Geometrical Configuration	Description
RP-C7-Dr35%	Raft over piles upper crust layer 7m relative density of sand 35%
R-C7-Dr35%	Raft upper crust layer 7m relative density of sand 35%
RP-C7-Dr55%	Raft on piles upper crust layer 7m relative density of sand 55%
R-C7-Dr55%	Raft upper crust layer 7m relative density of sand 55%.
RP-C7-Dr75%	Raft on piles upper crust layer 7m relative density of sand 75%
R-C7-Dr75%	Raft upper crust layer 7m relative density of sand 75%
RP-C4-Dr35%	Raft on piles upper crust layer 4m relative density of sand 35%
R-C4-Dr35%	Raft upper crust layer 4m relative density of sand 35%
RP-C4-Dr55%	Raft on piles upper crust layer 4m relative density of sand 55%
R-C4-Dr55%	Raft upper crust layer 4m relative density of sand 55%
RP-C4-Dr75%	Raft on piles upper crust layer 4m relative density of sand 75%
R-C4-Dr75%	Raft upper crust layer 4m relative density of sand 75%



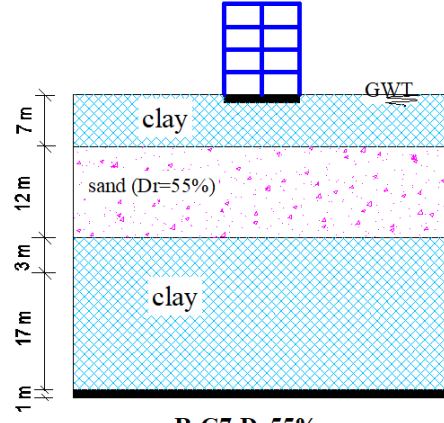
RP-C7-Dr35%



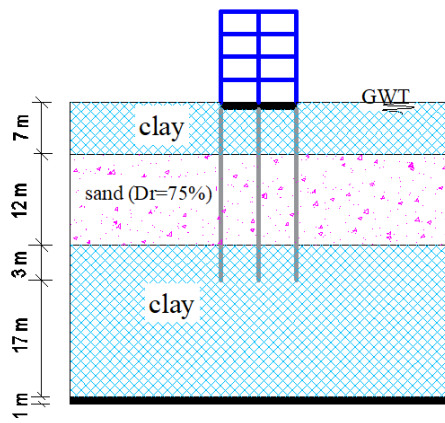
R-C7-Dr35%



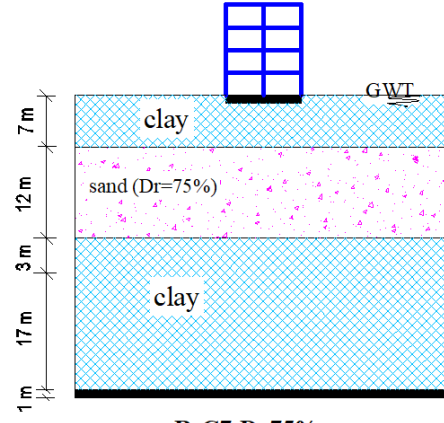
RP-C7-Dr55%



R-C7-Dr55%



RP-C7-Dr75%



R-C7-Dr75%

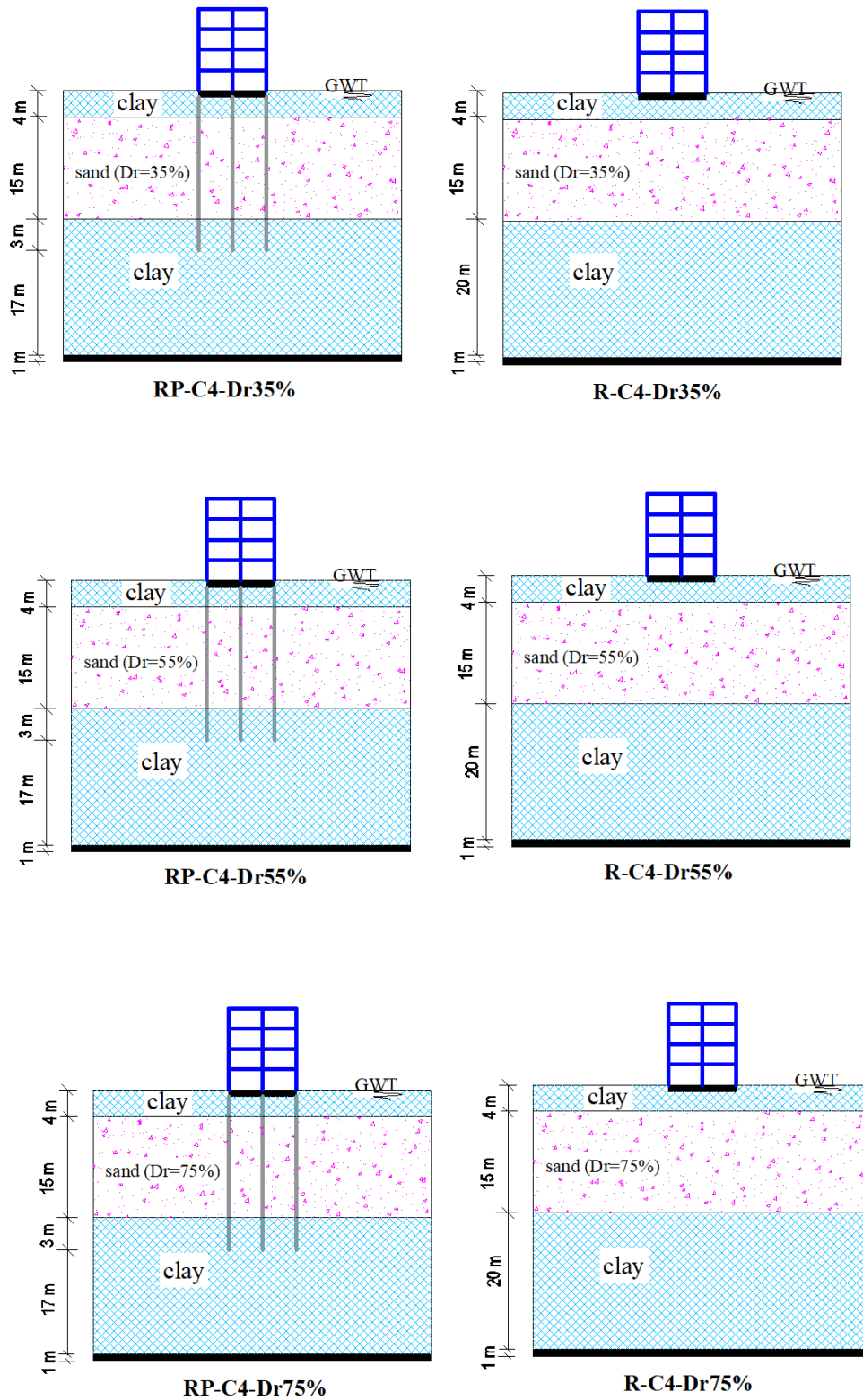


Figure 7. Geometric configurations analysed.

3.3. Constitutive model

This study employs a multi-material constitutive modeling approach to capture the behavior of the piled raft foundation system subjected to seismic loading. The PM4Sand model, a stress-ratio controlled, critical state compatible, bounding-surface plasticity model, is chosen to simulate the liquefaction behavior of the sand layer due to its well-established capabilities in this area (R. Boulanger and Ziotopoulou 2015), and (Dafalias and Manzari 2004). However, limitations exist in the PM4Sand model's ability to accurately represent initial stress conditions. To address this limitation, the Hardening Soil model with small-strain stiffness (HSS) is incorporated to determine the initial stresses within the soil profile accurately (Brinkgreve, Engin, and Engin 2010). This approach leverages the strengths of both models: PM4Sand for capturing liquefaction and HSS for representing initial stress conditions in both clay and sand. The input parameters for the raft and building are provided in Table 2, while those for the soils using the HSS model are presented in Table 4 and derived from formulas below and outlined in reference (Brinkgreve, Engin, and Engin 2010).

$$\gamma_{unsat} = 15 + 4.0Dr / 100 [Kn / m^3]$$

$$\gamma_{sat} = 19 + 1.6Dr / 100 [Kn / m^3]$$

$$E_{50}^{ref} = 60000Dr / 100 [Kn / m^2]$$

$$E_{oed}^{ref} = 60000Dr / 100 [Kn / m^2]$$

$$E_{ur}^{ref} = 180000Dr / 100 [Kn / m^2]$$

$$G_o^{ref} = 60000 + 68000Dr / 100 [Kn / m^2]$$

3.4. Superstructure

The building under investigation is a four-story structure with a basement, of a total height of 13 meters. The horizontal dimensions are specified as 10 meters wide. A uniform load of 5 kN/m² is assumed for both the floors and walls. The superstructure consists of four stories, each 3 meters height, shallow foundation with basement extends 1 meter below ground level is considered. Details regarding the material properties for Basement, floors, slab and walls are provided in Table 2. A noteworthy aspect of the model is the placement of columns at mid-span with node-to-node anchors, see Table 3. This configuration represents a worst-case scenario for earthquake-induced settlements. The decision to include a basement level serves to avoid unrealistic overestimations of total settlement that might occur if the structure were directly placed on the ground surface (Arboleda-Monsalve, Nguyen, and Center 2016). Material properties for the walls and floors are assumed to be linear elastic. Rayleigh damping is utilized to represent the material damping within the structure.

Table 2. Material Properties of building (Toma 2017),(Edition 2020)

Parameter	Name	Basement	Slab and floors	Walls	Unit
Material type	-	Elastic	Elastic	Elastic	-
Weight	w	20	10	5	kN/m/m
Rayleigh α	-	0.2320	0.2320	0.2320	-
Rayleigh β	-	8.0E-3	8.0E-3	8.0E-3	-
Axial stiffness	EA ₁	12.0E6	12.0E6	12.0E6	kN/m
Bending stiffness	EI	160.0E3	160.0E3	160.0E3	kNm ² /m

Table 3. Material Properties of columns

Parameter	Name	Column	Unit
Material type	Type	Elastic	-
Out-of-plane spacing	$L_{spacing}$	3	m
Axial stiffness	EA	2.50E6	kN

Table 4. Soil Parameters used in the numerical models (R. Boulanger and Ziotopoulou 2015)*, (Brinkgreve, Engin, and Engin 2010)** ,(Toma 2017)***

PM4Sand model*				(HSS) model**				Clay (HSS) model***
Symbol	DR=35 %	DR=55 %	DR=75 %	symbol	DR=35%	DR=55%	DR=75 %	
γ_{unsat} (kN/m ³)	16.4	17.2	18	γ_{unsat} (kN/m ³)	16.4	17.2	18	16
γ_{sat} (kN/m ³)	19.56	19.88	20.2	γ_{sat} (kN/m ³)	19.56	19.88	20.2	20
e	0.695	0.635	0.575	e	0.695	0.635	0.575	-
Dr	0.35	0.55	0.75	E_{50}^{ref} (kPa)	21000	33000	45000	20000
G ₀	476	677	890	E_{oed}^{ref} (kPa)	21000	33000	45000	25000
h _{p0}	0.53	0.4	0.63	E_{ur}^{ref} (kPa)	63000	99000	135000	80000
e _{max}	0.8	0.8	0.8	G_0^{ref} (kPa)	83800	97400	111000	180000
e _{min}	0.5	0.5	0.5	m	0.60	0.53	0.46	1
n ^d	0.1	0.1	0.1	c' (kPa)	0	0	0	10
n ^b	0.5	0.5	0.5	ϕ'	32	34	38	18
p _a (MPa)	0.1013	0.1013	101.3	ν	0.3	0.3	0.3	0.2
ϕ_{cv}	33	33	33	$\gamma_{0.7}$	1.65*10 ⁻⁴	1.45*10 ⁻⁴	1.25*10 ⁻⁴	0.12*10 ⁻³
ν	0.3	0.3	0.3	p^{ref} (kPa)	100	100	100	100
Q	10	10	10	R _f	0.956	0.931	0.91	0.9
R	1.5	1.5	1.5	K ₀	0.455	0.455	0.455	0.691

3.5. Analysis stages

The simulation process was divided into three distinct phases: (a) initial phase (Phase I), (b) building phase (Phase II), and (c) dynamic phase (Phase III).

- **Phase I:** The initial phase employed the K₀ procedure to establish the initial stress field within the model.

- **Phase II:** The second phase involved a plastic analysis by the Hardening Small Strain Model. This phase addressed the limitation of the PM4Sand model in accurately representing static conditions, in which plates, anchors, and basement interfaces are activated.
- **Phase III:** The final phase focused on the dynamic response of the system. The PM4Sand model was utilized for this analysis, along with an undrained A drainage type to simulate the development of excess pore pressure

4. Results and discussions

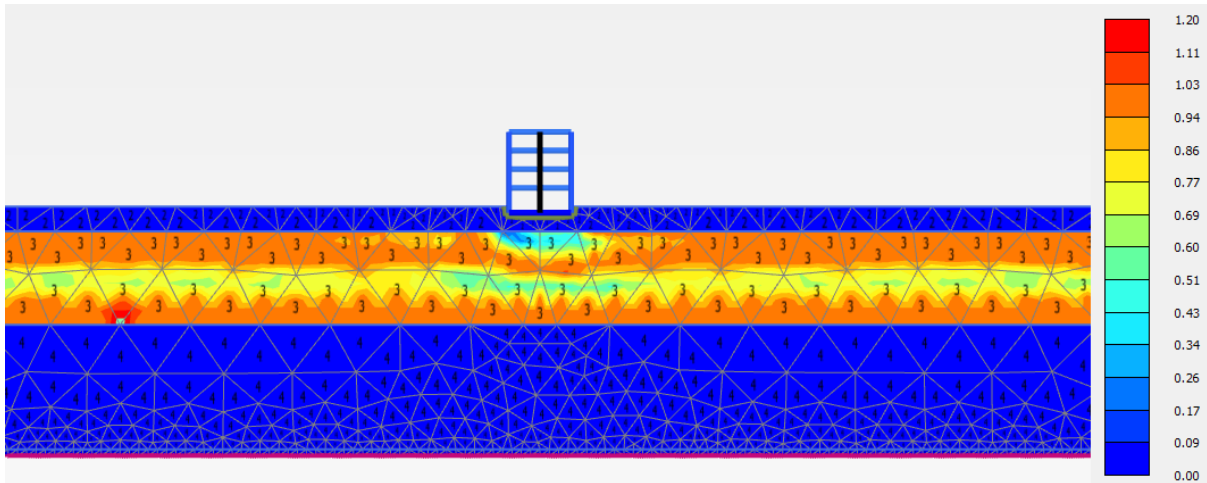
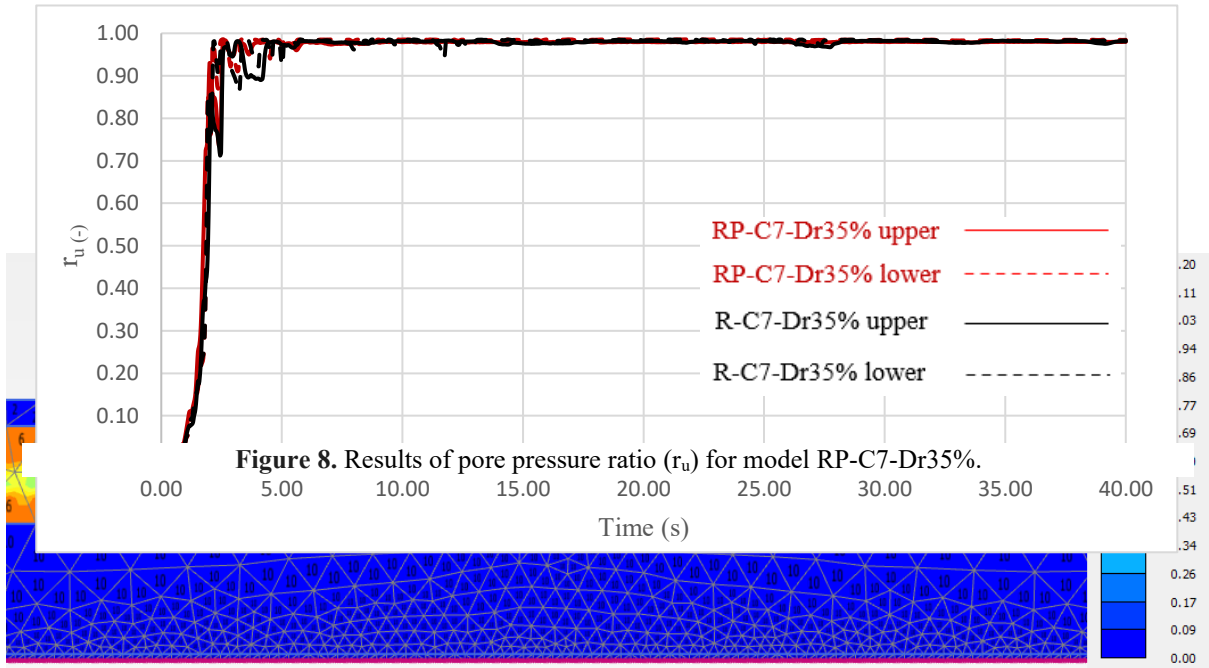
4.1. Pore pressure

Cyclic loading can induce soil liquefaction, a phenomenon characterized by a significant reduction in shear strength due to the accumulation of excess pore water pressure (Δu). This Δu reduces the effective stress (σ') within the soil, potentially leading to substantial deformations or complete failure. The severity of liquefaction is governed by the magnitude and duration of Δu , along with the initial soil properties and the specific loading conditions. A thorough understanding of these relationships is essential for evaluating liquefaction hazards and establishing safe design practices in earthquake-prone areas.

The excess pore water pressure ratio (r_u) can be calculated as follows:

$$r_u = 1 - \frac{\sigma_v}{\sigma_{vo}}$$

When $r_u = 0$, the effective stress is equal to the initial value, and the soil remains stable. Conversely, $r_u = 1$ indicates complete loss of effective stress, signifying liquefaction (assuming constant total stresses during cyclic loading). While true liquefaction occurs at $r_u = 1$, a value of $r_u \geq 0.8$ is often considered indicative of significant strain development and potential cyclic mobility based on previous research (Koutsourelakis, Prévost, and Deodatis 2002), (Montoya-Noguera and Lopez-Caballero 2016). Therefore, this study adopts $r_u = 0.8$ as the criterion for liquefaction triggering. Figures (11 to 14) illustrate the excess pore pressure time histories computed at the top and bottom of the liquefiable soil layer for both raft and piled raft foundation systems. The results reveal consistently higher r_u values for piled raft systems compared to raft foundations. This disparity is attributed to the contrasting vibration patterns in the upper soil induced by the inertial forces acting on the piles as shown in Fig.8. These forces generate larger shear strains in the surrounding soil, leading to a more pronounced increase in r_u . However, the difference diminishes with depth. In contrast to piled foundations, raft foundations as shown in Fig.9 distribute building loads uniformly across the entire foundation area, thereby increasing the overburden pressure and reducing susceptibility to liquefaction in the upper portion of the liquefiable soil layer. As shown in Figure 11, Model RP-C7-Dr55% reaches a pore pressure ratio of 80% within 2.44 seconds, suggesting imminent liquefaction. Model R-C7-Dr55% exhibits delayed liquefaction, achieving the same level of pore pressure after 3.88 seconds. The influence of foundation type on pore pressure ratio becomes more evident in models with a thinner upper clay crust (4m) as shown in Figure 12 Model RP-C4-Dr35% reached a maximum r_u of 97%, while Model R-C4-Dr35%, with a raft foundation, reached a lower 82%. Similar trend also observed in models RP-C4-Dr55% and R-C4-Dr55% as shown in figure 13.



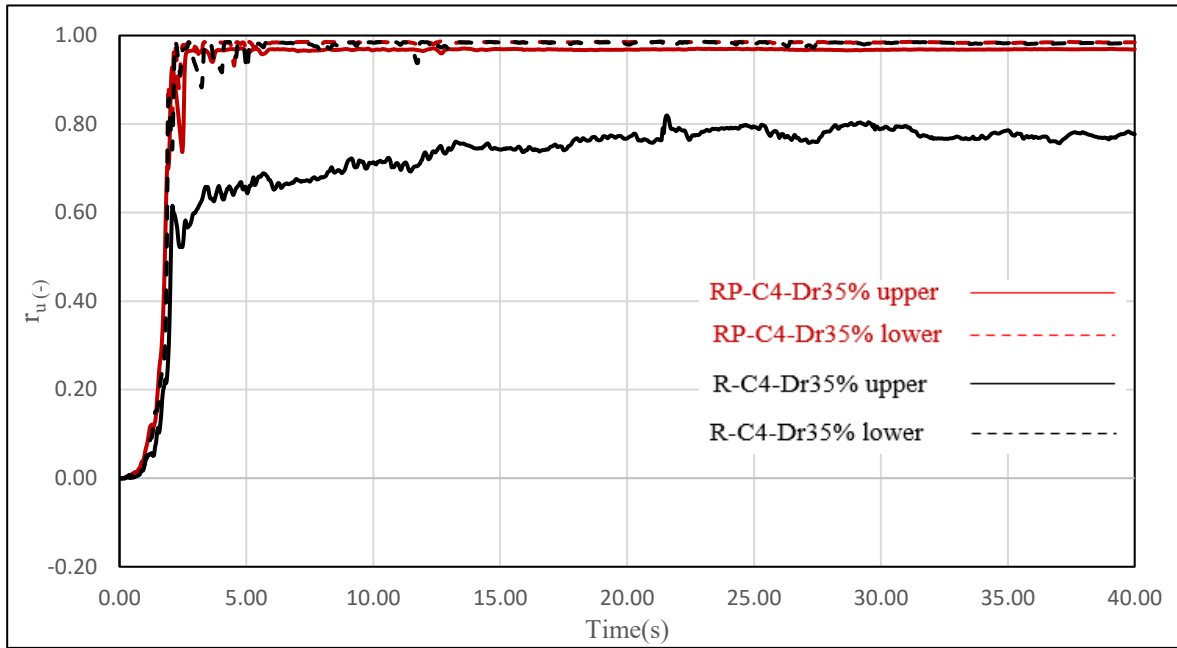


Figure 11. Results of pore pressure ratio (r_u) for model RP-C7-Dr55% and R-C7-Dr55%.

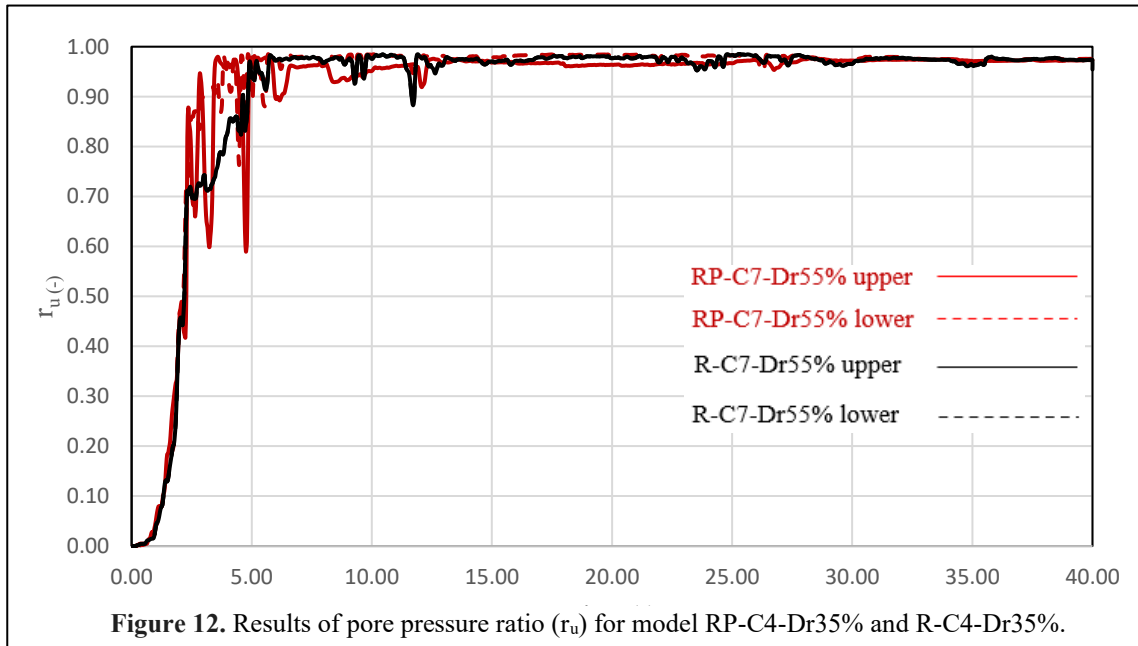


Figure 12. Results of pore pressure ratio (r_u) for model RP-C4-Dr35% and R-C4-Dr35%.

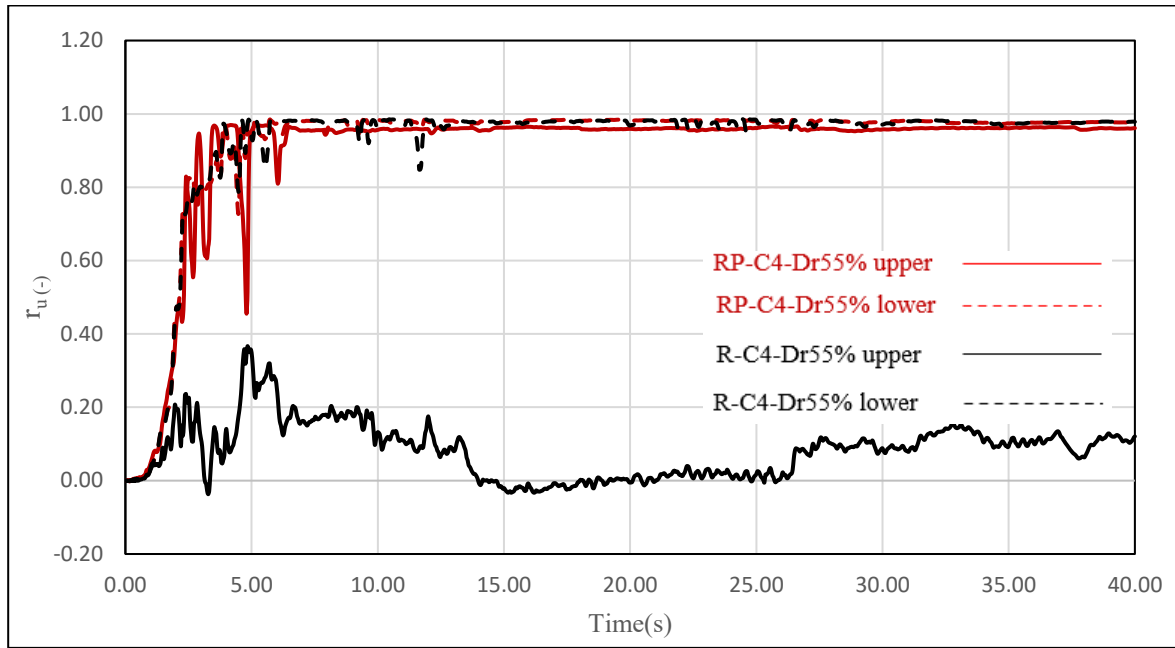


Figure 13. Results of pore pressure ratio (r_u) for model RP-C4-Dr55% and RP-C4-Dr55%.

Conclusion

- This investigation compared the pore-pressure ratio (r_u) in piled raft foundations as well as raft foundations. The results consistently indicated higher r_u values for piled raft systems. model RP-C7-Dr55% achieved a r_u of 80% after 2.3 seconds, whereas mode R-C7-Dr55% required 3.8 seconds to reach the same ratio. This disparity is attributed to the contrasting vibration patterns in the upper soil induced by the inertial forces acting on the piles. These forces generate larger shear strains in the surrounding soil, leading to a more pronounced increase in r_u .
- The difference in pore water pressure ratio between raft and piled raft foundations diminishes with increasing depth. This phenomenon can be attributed to the absence of inertial forces at greater depths within the soil. This observation underscores the critical importance of considering soil-structure interaction during foundation analysis.

Notation

γ_{unsat}	un-saturated unit weight
γ_{sat}	saturated unit weight
e	void ratio
Dr	relative density
G_0	shear modulus coefficient
h_{po}	contraction rate parameter
e_{max}	maximum void ratio

e_{min}	minimum void ratio
n^d	Dilatancy surface parameter
n^b	Bounding surface parameter
P_a	atmospheric pressure
ϕ_{cv}	critical state friction angle
ν	Poisson ratio
Q, R	Bolton's critical state parameters
E_{50}^{ref}	secant stiffness modulus
E_{oed}^{ref}	tangent stiffness modulus
E_{ur}^{ref}	unloading reloading stiffness modulus
m	rate of stress dependency
c'	effective cohesion
ϕ'	effective friction angle
$\gamma_{0.7}$	shear strain ratio
G_0^{ref}	reference shear modulus at very small strains
p^{ref}	reference stress level
R_f	failure ratio
k	Permeability

Funding No funding was obtained.

Availability of data and materials Paper doesn't contain all data used in the study for more data contact with the *Corresponding author*.

Declaration of competing interest the authors state that they have no known competing financial interests or personal relationships that could have influenced the work described in this study.

References

- Abdoun, T H. 1998. "Seismically Induced Lateral Spreading of Two-Layer Sand Deposit and Its Effect on Pile Foundations." *Proc. Centrifuge 98*: 321–26.
- Abdoun, Tarek, and Ricardo Dobry. 2002. "Evaluation of Pile Foundation Response to Lateral Spreading." *Soil Dynamics and Earthquake Engineering* 22(9–12): 1051–58.
- Arboleda-Monsalve, Luis G, Hung M Nguyen, and METRANS Transportation Center. 2016. "Simulation of Liquefaction-Induced Damage of the Port of Long Beach Using the UBC3D-PLM Model: Final Report [2017]."
- Ashour, Mohamed, and Gary Norris. 2003. "Lateral Loaded Pile Response in Liquefiable Soil." *Journal of Geotechnical and Geoenvironmental Engineering* 129(5): 404–14.
- Bhattacharya, Subhamoy, S P G Madabhushi, and M D Bolton. 2004. "An Alternative Mechanism of Pile Failure

- in Liquefiable Deposits during Earthquakes.” *Geotechnique* 54(3): 203–13.
- Boulanger, Ross W et al. 1999. “Seismic Soil-Pile-Structure Interaction Experiments and Analyses.” *Journal of geotechnical and geoenvironmental engineering* 125(9): 750–59.
- Boulanger, Ross, and Katerina Ziotopoulou. 2015. *PM4Sand Version 3: A Sand Plasticity Model for Earthquake Engineering Applications*.
- Brinkgreve, R, Erjona Engin, and Harun Kürşat Engin. 2010. *Validation of Empirical Formulas to Derive Model Parameters for Sands*.
- Dafalias, Yannis F, and Majid T Manzari. 2004. “Simple Plasticity Sand Model Accounting for Fabric Change Effects.” *Journal of Engineering mechanics* 130(6): 622–34.
- Dobry, R, V Taboada, and L Liu. 1997. “Centrifuge Modeling of Liquefaction Effects during Earthquakes.” In *Earthquake Geotechnical Engineering*, , 1291–1324.
- Dungca, Jonathan R et al. 2006. “Shaking Table Tests on the Lateral Response of a Pile Buried in Liquefied Sand.” *Soil Dynamics and Earthquake Engineering* 26(2–4): 287–95.
- Edition, Connect. 2020. “CONNECT Edition V20.02.”
- Han, J T, S R Kim, J I Hwang, and M M Kim. 2007. “Evaluation of the Dynamic Characteristics of Soil-Pile System in Liquefiable Ground by Shaking Table Tests.” In *4th International Conference on Earthquake Geotechnical Engineering*, Thessaloniki, Greece.
- Horikoshi, Kenichi, Akira Tateishi, and Tadafumi Fujiwara. 1998. “Centrifuge Modeling of a Single Pile Subjected to Liquefaction-Induced Lateral Spreading.” *Soils and Foundations* 38: 193–208.
- Koutsourelakis, Steve, Jean H Prévost, and George Deodatis. 2002. “Risk Assessment of an Interacting Structure–Soil System Due to Liquefaction.” *Earthquake engineering & structural dynamics* 31(4): 851–79.
- López Jiménez, Guillermo A, Daniel Dias, and Oriane Jenck. 2019. “Effect of the Soil–Pile–Structure Interaction in Seismic Analysis: Case of Liquefiable Soils.” *Acta Geotechnica* 14(5): 1509–25.
- Montoya-Noguera, Silvana, and Fernando Lopez-Caballero. 2016. “Effect of Coupling Excess Pore Pressure and Deformation on Nonlinear Seismic Soil Response.” *Acta Geotechnica* 11: 191–207.
- Satoh, H, N Ohbo, and K Yoshizako. 1998. “Dynamic Test on Behavior of Pile during Lateral Ground Flow.” In *Centrifuge 98*, , 327–32.
- Suzuki, Hiroko, Kohji Tokimatsu, Masayoshi Sato, and Akio Abe. 2006. “Factor Affecting Horizontal Subgrade Reaction of Piles during Soil Liquefaction and Lateral Spreading.” In *Seismic Performance and Simulation of Pile Foundations in Liquefied and Laterally Spreading Ground*, , 1–10.
- Takahashi, A. 1998. “Stability of Piled Pier Subjected to Lateral Flow Soils during Earthquake.” *Proc. of Centrifuge '98 (IS-Tokyo '98)*: 365–76.
- Tamura, Shuji, and Kohji Tokimatsu. 2006. “Seismic Earth Pressure Acting on Embedded Footing Based on Large-Scale Shaking Table Tests.” In *Seismic Performance and Simulation of Pile Foundations in Liquefied and Laterally Spreading Ground*, , 83–96.
- Tokimatsu, Kohji, Hiroko Suzuki, and Masayoshi Sato. 2005. “Effects of Inertial and Kinematic Interaction on Seismic Behavior of Pile with Embedded Foundation.” *Soil Dynamics and Earthquake Engineering* 25(7–10): 753–62.
- Toma, Mohsin Ara. 2017. “Earthquake Response Analysis of Pile Supported Structures–Correspondence of PLAXIS 2D with Eurocode 8.”
- Towhata, I, W Vargas-Monge, R P Orense, and M Yao. 1999. “Shaking Table Tests on Subgrade Reaction of Pipe Embedded in Sandy Liquefied Subsoil.” *Soil Dynamics and Earthquake Engineering* 18(5): 347–61.
- Wilson, Daniel Wayne. 1998. *Soil-Pile-Superstructure Interaction in Liquefying Sand and Soft Clay*. University of California, Davis America.
- Yao, Shintaro, Koichi Kobayashi, Nozomu Yoshida, and Hiroshi Matsuo. 2004. “Interactive Behavior of Soil–Pile-Superstructure System in Transient State to Liquefaction by Means of Large Shake Table Tests.” *Soil Dynamics and Earthquake Engineering* 24(5): 397–409.